Table II. Formal Reduction Potentials (V vs NHE) of Pentaammineruthenium(III) Complexes of σ- and π-Donor Ligands

complex	$E_f(Ru^{3+/2+})$
$Ru(NH_3)_6^{3+}$	0.050[a]
$Ru(NH_3)_5(OH_2)^{2+}$	0.067[a]
$Ru(NH_3)_5(imidazole)^{3+}$	0.079[b]
$Ru(NH_3)_5(cytidine)^{3+}$	0.09[c]
$Ru(NH_3)_5(2,3\text{-}Cl_2Hpcyd)^{3+}$	0.451[d]
$Ru(NH_3)_5(NCS)^{2+}$	0.133[e]
$Ru(NH_3)_5Cl^{2+}$	-0.040[a]
$Ru(NH_3)_5Br^{2+}$	-0.020[a]
$Ru(NH_3)_5(2,3\text{-}Cl_2pcyd)^{2+}$	-0.095[d]
$Ru(NH_3)_5(cytidine\ anion)^{2+}$	-0.30[f]
$Ru(NH_3)_5(OH)^{2+}$	-0.420[e]

[a] Aqueous solution of 0.10 M *p*-toluenesulfonic acid/0.10 M potassium *p*-toluenesulfonate: Matsubara, T.; Ford, P. C. *Inorg. Chem.* **1976**, *15*, 1107 and ref 34. [b] Aqueous solution of 0.1 M phosphate buffer plus 0.9 M $NaClO_4$: Johnson, C. R.; Shepherd, R. E. *Synth. React. Inorg. Met.-Org. Chem.* **1984**, *14*, 339. [c] Aqueous solution, 0.01 M $HClO_4$ + 0.09 M $LiClO_4$: Clarke, M. J. *J. Am. Chem. Soc.* **1978**, *100*, 5068. [d] Acetonitrile solution: this work. [e] Aqueous solution of 0.2-1 M NaOH: Lim, H. S.; Barklay, D. J.; Anson, F. C. *Inorg. Chem.* **1972**, *7*, 1460. [f] Aqueous solution, 0.1 M LiOH: Clarke, M. J. *J. Am. Chem. Soc.* **1978**, *100*, 5068.

pentaammineruthenium(III) complexes of π-donor ligands in Table II. Pentaammineruthenium(III) is a strong π acid, and its oxidation state should be stabilized by a strong π-donor ligand. Therefore, it should be possible to relate increasingly negative reduction potentials to the π-donor strength of a ligand. However, as the data in Table II illustrate, great care should be taken in interpretation. While NH_3 has no π-donor properties and water is a weak π donor, the reduction potential of $[Ru(NH_3)_6]^{3+}$ is more negative than that of $[Ru(NH_3)_5(H_2O)]^{3+}$. Clearly, the overall donicity of the ligand is important in determining reduction potential. The ligands thiocyanate and 2,3-Cl_2Hpcyd are π donors to ruthenium(III) but function as π acids to ruthenium(II). Thus, the reduction potentials in Table II reflect the stabilization of the ruthenium(II) oxidation state by π-acid ligands. The ligands Cl^-, Br^-, 2,3-Cl_2pcyd$^-$, cytidine anion, and OH^- are both σ and π donors with little π-acid properties. The slight anodic shift in reduction potentials in going from Cl^- to Br^- seems counterintuitive as Br^- is more polarizable and should be a better π donor. One possible explanation[34] is that the smaller size of the π orbitals of Cl^- compared to Br^- permits greater effective overlap with the ruthenium(III) πd orbitals. For the nitrogen-bound cytidine anion and OH^- ligands, the match in size between π orbitals may be far better. This is supported by pK_a measurements of coordinated water in $[Rh(NH_3)_5(H_2O)]^{3+}$ (pK_a = 6.8)[35] and $[Ru(NH_3)_5(H_2O)]^{3+}$ (pK_a = 4.2).[33] Rh(III) has a low-spin d^6 configuration in which all the πd orbitals are filled and, therefore, can only σ bond to H_2O or OH^-. The difference in pK_a of water coordinated to ruthenium and rhodium in these complexes is a measure of the importance of π bonding in the ruthenium(III) complex.[36] The anionic cyanamide ligand appears to be a significantly better π donor ligand than Cl^- and Br^- but less so than cytidine anion or OH^-. It should be possible to increase the cyanamide ligand π-donor properties by substituting electron-donor substituents on the phenyl ring. Future studies will attempt to quantitatively evaluate the importance of π bonding in phenylcyanamide ligands.

Acknowledgment. R.J.C. acknowledges the Natural Sciences and Engineering Research Council of Canada for their financial support and an NSERC University Research Fellowship.

Registry No. 2,3-Cl_2Hpcyd, 71232-27-4; $[(NH_3)_5Ru(Cl)][Cl]_2$, 18532-87-1; $[(NH_3)_5Ru(H_2O)][PF_6]_2$, 34843-18-0; $[(NH_3)_5Ru(2,3\text{-}Cl_2pcyd)][ClO_4]_2$, 120204-95-7; $[(NH_3)_5Ru(2,3\text{-}Cl_2pcyd)][ClO_4]_3$, 120204-97-9; Tl(2,3-$Cl_2$pcyd), 120204-98-0; ammonium thiocyanate, 1762-95-4; benzoyl chloride, 98-88-4; 2,3-dichloroaniline, 608-27-5.

(34) Marchant, J. A.; Matsubara, T.; Ford, P. C. *Inorg. Chem.* **1977**, *16*, 2160.
(35) Palmer, D. A.; Harris, G. M. *Inorg. Chem.* **1974**, *13*, 965.
(36) It is assumed that there is little difference in effective charge between Ru(III) and Rh(III).

Contribution from the Dipartimento di Chimica, Università di Firenze, Firenze, Italy, and Istituto per lo Studio della Stereochimica ed Energetica dei Composti di Coordinazione del CNR, Firenze, Italy

Crystal and Molecular Structure and Magnetic Properties of the μ-Azido-Bridged Low-Spin Cobalt(II) Complex $[(CH_3C(CH_2PPh_2)_3)Co(\mu\text{-}N_3)]_2(BPh_4)_2\cdot 2(CH_3)_2CO$

Alessandro Bencini,*[1a] Carlo A. Ghilardi,[1b] Stefano Midollini,[1b] and Annabella Orlandini[1b]

Received August 24, 1988

The complex $[(triphos)Co(\mu\text{-}N_3)]_2(BPh_4)_2\cdot 2(CH_3)_2CO$, triphos = $CH_3C(CH_2PPh_2)_3$, crystallizes in the triclinic system, space group $P\bar{1}$, with a = 18.122 (9) Å, b = 14.025 (8) Å, c = 12.668 (7) Å, α = 92.95 (8)°, β = 103.77 (9)°, and γ = 108.12 (8)°. The molecular structure consists of discrete dinuclear $[(triphos)Co(\mu\text{-}N_3)]_2^{2+}$ cations with the cobalt atoms in a distorted P_3N_2 square-pyramidal environment. The compound is diamagnetic, and the observed diamagnetism has been related to the low-symmetry mixing of $d_{x^2-y^2}$ orbitals of cobalt with the ground d_{z^2} orbitals by using extended Hückel calculations. With the same model the magnetic properties of related azido-bridged nickel(II) complexes have been rationalized.

Introduction

During the last few years a number of μ-azido-bridged dinuclear complexes have been synthesized with the aim of investigating their magnetic properties.[2,3] The actual type of bridging arrangement that one can obtain from the azido ions is not easily predictable, but the magnetic properties of the resulting solid are strongly dependent on the bridging mode of N_3^-. The coordination chemistry of the N_3^- ion is, in this sense, rather different from that of other groups or ions that bridge transition-metal ions to form di- or polynuclear systems.[4] The oxalato ion, for example, always bridges two metals like a bis-chelating donor and transmits antiferromagnetic exchange interactions.[5] The largest number

(1) (a) University of Florence. (b) CNR.
(2) Kahn, O. In *Magneto Structural Correlations in Exchange Coupled Systems*; Willett, R. D., Gatteschi, D., Kahn, O., Eds.; Reidel: Dordrecht, The Netherlands, 1985; p 57.
(3) Cairns, C. J.; Bush, D. H. *Coord. Chem. Rev.* **1986**, *69*, 1.
(4) Hendrickson, D. N. In *Magneto Structural Correlations in Exchange Coupled Systems*; Willett, R. D., Gatteschi, D., Kahn, O., Eds.; Reidel: Dordrecht, The Netherlands, 1985; p 523.

0020-1669/89/1328-1958$01.50/0

of μ-azido-bridged complexes reported so far contain copper(II) ions. In these complexes N_3^- ions generally form double bridges of the types[6,7]

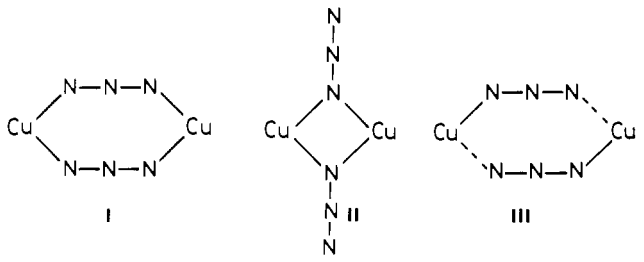

In type I complexes the N_3^- ions bridge the copper atoms in a symmetrical fashion. One example is found of a dinuclear copper(II) cryptate of a macrocyclic ligand. In this case the copper(II) ions are six-coordinate and the complex is diamagnetic.[8] The diamagnetism of this complex has been ascribed to a very effective exchange pathway through the ground $d_{x^2-y^2}$ orbitals on copper and p orbitals of the azido groups.[9,10] Type II complexes have been obtained with either four- or six-coordinate copper(II) ions.[7,11] In both cases the triplet, $S = 1$, state is stabilized by ≈ 100 cm^{-1} with respect to the singlet, $S = 0$, state as confirmed by both magnetic susceptibility measurements and single-crystal EPR spectra.[12]

Type III complexes show a negligible interaction when the geometry around the metals is square-pyramidal[13] or a weak antiferromagnetic interaction when the geometry approaches the trigonal-bipyramidal limit.[9,14] The five-coordinate complex bis(μ-1,3-azido)bis(1,1,4,7,7-pentamethyldiethylenetriamine)dicopper(II) bis(tetraphenylborate), $Cu_2(Me_5dien)_2(N_3)_2(BPh_4)_2$, shows a rather small coupling ($J \approx 13$ cm^{-1}).[15] The coordination environment around copper is intermediate between a square pyramid and a trigonal bipyramid, and single-crystal EPR spectra[14] showed that the ground state is almost $d_{x^2-y^2}$. The N_3^- ions bridge the copper centers in axial-equatorial positions, giving rise to a less efficient exchange pathway.

The exchange interactions transmitted by azido ions in copper(II) complexes have been extensively studied by Kahn et al.[2,9,10]

Among the other metals of the transition series only nickel(II) complexes with bridging N_3^- have been magnetically characterized.[4,16] In all cases antiferromagnetic exchange interactions were observed. The largest couplings have been observed in $[LNi(\mu\text{-}N_3)_3NiL]ClO_4$ (L = *N,N',N''*-trimethyl-1,4,7-triazacyclononane), a complex with three bridging N_3^- groups, and in $[L'Ni(N_3)(\mu\text{-}N_3)_2Ni(N_3)L']$ (L' = 1,5,9-triazacyclododecane).[16] The observed J values were $J \approx 140$ cm^{-1} and $J \approx 180$ cm^{-1}, respectively. In six- and five-coordinate nickel(II) complexes both $d_{x^2-y^2}$ and d_{z^2} orbitals are involved in the exchange mechanism and additional information is needed to explain the nature of the magnetic interactions. A more complex situation is of course expected for manganese(II) or iron(II) complexes in which other d orbitals participate in the exchange mechanism.

In our laboratory some of us obtained a series of complexes of general formula $[(triphos)CoX]_2(BPh_4)_2$ (triphos = $CH_3C(CH_2PPh_2)_3$, X = Cl, Br, OH).[17] In these complexes the cobalt(II) ions are in the low-spin state in a slightly distorted square-pyramidal environment. This geometry suggests that the ground magnetic orbitals are mainly d_{z^2} in nature, and antiferromagnetic exchange interactions with J in the range 100–300 cm^{-1} have been measured.

We wish to report here the synthesis, the crystal and molecular structure, and the magnetic properties of $[(triphos)Co(\mu\text{-}N_3)]_2(BPh_4)_2\cdot 2(CH_3)_2CO$ with the aim to have a better insight into the mechanism of exchange interactions propagated through N_3^- bridging ions. The exchange pathways expected for the present complex will be investigated by using extended Hückel calculations. The same model will be also applied to rationalize the exchange interactions observed in μ-N_3-bridged nickel(II) complexes.

During the synthetic procedure crystals of composition $(triphos)Co(N_3)_2$ were also obtained, and their synthesis is also described here.

Table I. Crystallographic Data for $[(triphos)Co(\mu\text{-}N_3)]_2(BPh_4)_2\cdot 2(CH_3)_2CO$

$C_{136}H_{130}B_2Co_2N_6O_2P_6$	fw = 2205.9
a = 18.122 (9) Å	space group $P\bar{1}$
b = 14.025 (8) Å	T = 22 °C
c = 12.668 (7) Å	λ = 0.7107 Å
α = 92.95 (8)°	ρ_{calcd} = 1.244 g cm^{-3}
β = 103.77 (9)°	μ = 4.13 cm^{-1}
γ = 108.12 (8)°	$R(F_o)$ = 0.070
V = 2944.5 Å^3	$R_w(F_o)$ = 0.071
Z = 1	

Table II. Final Positional Parameters (×10^4)

atom	x	y	z
Co	1235 (1)	1269 (1)	1316 (1)
P1	1232 (1)	2859 (2)	1099 (2)
P2	1642 (1)	1627 (2)	3134 (2)
P3	2504 (1)	1663 (2)	1267 (2)
N1	197 (5)	461 (7)	1496 (7)
N2	−362 (6)	−4 (7)	772 (7)
N3	−939 (5)	−450 (7)	76 (7)
C1	3485 (5)	4401 (6)	3394 (7)
C2	2792 (5)	3435 (6)	2763 (6)
C3	2108 (5)	3782 (6)	2098 (7)
C4	2541 (5)	2765 (6)	3639 (6)
C5	3146 (5)	2905 (6)	2031 (7)
B	3630 (6)	6924 (7)	6236 (8)
C6[a]	4025 (13)	6717 (15)	1578 (18)
C7[a]	3320 (12)	6530 (13)	764 (16)
C8[a]	3231 (11)	6937 (14)	−303 (16)
O[a]	2677 (7)	6200 (9)	1053 (9)

[a] Atoms belonging to the solvent molecule.

Experimental Section

Synthesis of the Complexes. $[(triphos)Co(N_3)]_2(BPh_4)_2\cdot 2(CH_3)_2CO$. $[Co(H_2O)_6](ClO_4)_2$ (366 mg, 1 mmole dissolved in 15 cm^3 of 1-butanol was added to a solution of triphos (620 mg, 1 mmol) in 25 cm^3 of CH_2Cl_2. To the resulting solution was added a solution of NaN_3 (65 mg, 1 mmol) in 10 cm^3 of methanol. All these operations were carried out under an atmosphere of nitrogen at room temperature. Addition of solid $NaBPh_4$ (320 mg, 1 mmol) and evaporation of the solvent in a current of nitrogen led to the formation of large dark crystals of the title compound. Anal. Calcd for $[(triphos)Co(N_3)]_2(BPh_4)_2\cdot 2(CH_3)_2CO$: N, 3.81; C, 74.05; H, 5.94. Found: N, 4.00; C, 72.98; H, 5.74.

$[(triphos)Co(N_3)_2]$. The complex was prepared following a procedure similar to that described above by adding 2 mmol of NaN_3. Anal. Calcd for $[(triphos)Co(N_3)_2]$): N, 11.12; C, 63.58; H, 5.20. Found: N, 10,87; C, 63.92; H, 5.00.

X-ray Data Collection and Structure Determination. Single-crystal diffraction data for $[(triphos)Co(N_3)]_2(BPh_4)_2\cdot 2(CH_3)_2CO$ were collected at room temperature on a Philips PW1100 automated diffrac-

(5) Bencini, A.; Benelli, C.; Gatteschi, D.; Zanchini, C.; Fabretti, A. C.; Franchini, G. C. *Inorg. Chim. Acta* **1984**, *86*, 169.
(6) Dori, Z.; Ziolo, R. *Chem. Rev.* **1973**, *73*, 247.
(7) Comarmond, J.; Plumeré, P.; Lehn, J. M.; Agnes, Y.; Louis, R.; Weiss, R.; Kahn, O.; Morgenstern-Badarau, I. *J. Am. Chem. Soc.* **1982**, *104*, 6330.
(8) Agnes, Y.; Louis, R.; Gisselbrecht, J. P.; Weiss, R. *J. Am. Chem. Soc.* **1984**, *106*, 93.
(9) Kahn, O. In *Magneto Structural Correlations in Exchange Coupled Systems*; Willett, R. D., Gatteschi, D., Kahn, O., Eds.; Reidel: Dordrecht, The Netherlands, 1985; p 37.
(10) Charlot, M. F.; Kahn, O.; Chaillet, M.; Larrieu, C. *J. Am. Chem. Soc.* **1986**, *108*, 2574.
(11) Sikorav, S.; Bkouche-Waksman, I.; Kahn, O. *Inorg. Chem.* **1984**, *23*, 490.
(12) Boillot, M. L.; Journaux, Y.; Bencini, A.; Gatteschi, D.; Kahn, O. *Inorg. Chem.* **1985**, *24*, 263.
(13) Bkouche-Waksman, I.; Sikorav, S.; Kahn, O. *J. Crystallogr. Spectrosc. Res.* **1983**, *12*, 303.
(14) Felthouse, T. R.; Hendrickson, D. N. *Inorg. Chem.* **1978**, *17*, 444.
(15) Banci, L.; Bencini, A.; Gatteschi, D. *Inorg. Chem.* **1984**, *23*, 2138.
(16) Chauduri, P.; Guttman, M.; Ventur, D.; Wieghardt, K.; Nuber, B.; Weiss, J. *J. Chem. Soc., Chem. Commun.* **1985**, 1618.
(17) Mealli, C.; Midollini, S.; Sacconi, L. *Inorg. Chem.* **1975**, *14*, 2513.

Table III. Parameters Used in the Extended Hückel Calculations

atom	orbital type	VSIP	c_1	ζ_1	c_2	ζ_2
Co	3d	−13.18	0.5933	5.95	0.5744	2.30
	4s	−9.21	1.0000	2.22		
	4p	−5.29	1.0000	2.22		
P	3s	−18.60	1.0000	1.60		
	3p	−14.00	1.0000	1.60		
N	2s	−26.00	1.0000	1.95		
	2p	−13.4	1.0000	1.95		
H	1s	−13.6	1.0000	1.30		

tometer. The cell dimensions were determined by the least-squares refinement of 24 carefully centered reflections. Details of crystal data and intensity data collection are given in Table I. The intensities of three standard reflections measured every 2 h were used to rescale the observed intensities to account for the decay of ca. 15%. The standard deviations of the observed intensities, $\sigma(I)$, were calculated by using the value of 0.03 for the instability factor k.[18] The intensities were corrected for Lorentz–polarization effects.[19a] Owing to the irregular shape of the crystals, no absorption correction was applied. An empirical estimation of the effects of absorption on several reflections showed the largest change in intensities within ±10%.

The structure was solved by the heavy-atom method. The refinement was based on F_o, the function minimized being $\sum w(|F_o| - |F_c|)^2$, where $w = 1/\sigma^2(F_o)$. Full-matrix least-squares refinements were carried out by using anisotropic thermal parameters for cobalt, phosphorus, and nitrogen atoms and isotropic thermal parameters for the other atoms. The phenyl rings were treated as rigid groups. The hydrogen atoms were introduced in calculated positions but not refined. At convergence final R and R_w factors defined as $R = \sum||F_o| - |F_c||/\sum|F_o|$ and $R_w = [\sum w(|F_o| - |F_c|)^2/\sum w(F_o)^2]^{1/2}$ were 0.070 and 0.071, respectively. All the crystallographic calculations were performed on a SEL 32/77 computer by using SHELX-76 and ORTEP programs.[19] Atomic scattering factors of the neutral atoms were taken from ref 20. Both the f' and f'' of the anomalous dispersion correction were included for the non-hydrogen atoms.[21]

The positional parameters for the non-hydrogen atoms are reported in Table II. Complete crystallographic data and data collection details (Table SI), derived positional parameters for atoms in rigid groups (Table SII), calculated positional parameters for hydrogen atoms (Table SIII), thermal parameters for non-hydrogen atoms (Table SIV), and a complete listing of the observed and calculated structure factors are given as supplementary material.

Computational Details. Extended Hückel calculations[22] have been performed by using the FORTICON program properly modified to include a fragment molecular orbital basis. The nondiagonal elements H_{ij} of the Hückel matrix have been computed through the relationship $H_{ij} = 1.75S_{ij}(H_{ii} + H_{jj})/2$, where S_{ij} is the overlap integral between the ϕ_i and ϕ_j atomic orbitals. Atomic orbitals of Slater type were used by taking single-ζ radial functions for all the atomic orbitals except 3d cobalt functions, for which a double-ζ basis was used. The calculations were performed on the model complex $\{[(PH_3)_3Co]_2(N_3)_2\}^{2+}$ with an idealized C_{2h} symmetry. The bond angles around the metal atoms were fixed at 90°. The following bond distances have been used: Co–P_{eq} = 2.21 Å, Co–P_{ax} = 2.26 Å, Co–N = 1.93 Å, N–N = 1.13 Å, P–H = 1.08 Å. The actual values of the VSIP and coefficients and exponents of the Slater functions are collected in Table III. All the calculations were performed on a IBM Personal System 2 computer.

Magnetic Measurements. The temperature dependence of the magnetic susceptibility was measured on polycrystalline samples in the temperature range 4.2–300 K. The measurements were performed by using an automated DSM5 susceptometer equipped with an Oxford Instruments CF1200S continuous-flow cryostat. $CoHg(NCS)_4$ was used as a calibrant of the magnetic field and of the temperature by using the data in ref 23.

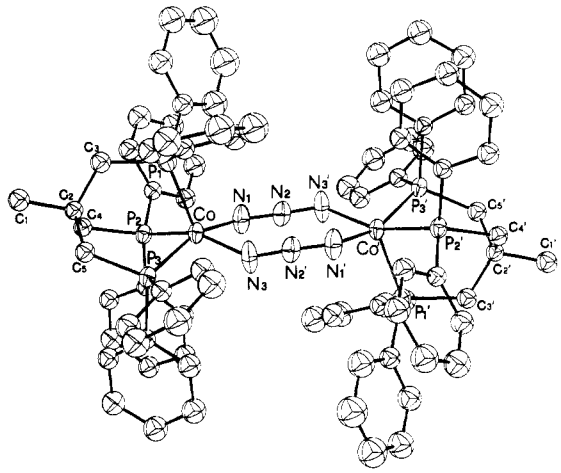

Figure 1. ORTEP view of the dinuclear cation $[(triphos)Co(\mu\text{-}N_3)]_2^{2+}$.

Table IV. Selected Bond Distances (Å) and Angles (deg)

Co–P1	2.261 (3)	P2–C4	1.843 (7)
Co–P2	2.223 (3)	P2–C1,3	1.830 (6)
Co–P3	2.207 (3)	P2–C1,4	1.819 (7)
Co–N1	1.945 (9)	P3–C5	1.831 (7)
Co–N3	1.917 (9)	P3–C1,5	1.820 (7)
N1–N2	1.174 (10)	P3–C1,6	1.824 (7)
N2–N3	1.166 (10)	C1–C2	1.551 (10)
P1–C3	1.843 (7)	C2–C3	1.550 (12)
P1–C1,1	1.821 (8)	C2–C4	1.549 (12)
P1–C1,2	1.821 (8)	C2–C5	1.527 (14)
P1–Co–P2	92.7 (1)	C4–P2–C1,4	105.4 (3)
P1–Co–P3	92.2 (1)	C1,3–P2–C1,4	102.3 (3)
P1–Co–N1	109.1 (3)	Co–P3–C5	113.3 (3)
P1–Co–N3	111.0 (3)	Co–P3–C1,5	109.1 (2)
P2–Co–P3	89.7 (1)	Co–P3–C1,6	120.7 (2)
P2–Co–N1	86.7 (2)	C5–P3–C1,5	110.4 (3)
P2–Co–N3	156.3 (3)	C5–P3–C1,6	102.1 (3)
P3–Co–N1	158.5 (3)	C1,5–P3–C1,6	100.4 (3)
P3–Co–N3	87.9 (3)	Co–N1–N2	124.5 (8)
N1–Co–N3	86.9 (4)	N1–N2–N3	176.9 (14)
Co–P1–C3	109.8 (3)	Co–N3–N2	139.4 (9)
Co–P1–C1,1	122.2 (2)	C1–C2–C3	107.2 (7)
Co–P1–C1,2	113.1 (2)	C1–C2–C4	106.4 (6)
C3–P1–C1,1	102.7 (4)	C1–C2–C5	106.5 (7)
C3–P1–C1,2	107.2 (3)	C3–C2–C4	113.4 (7)
C1,1–P1–C1,2	100.4 (3)	C3–C2–C5	112.7 (7)
Co–P2–C4	113.6 (3)	C4–C2–C5	110.1 (7)
Co–P2–C1,3	113.9 (2)	C2–C3–P1	120.0 (6)
Co–P2–C1,4	114.2 (2)	C2–C4–P2	115.9 (5)
C4–P2–C1,3	106.4 (3)	C2–C5–P3	117.6 (5)

Results and Discussion

Synthesis and Structure. The reaction of $[Co(H_2O)_6](ClO_4)_2$ and triphos with NaN_3 in equimolar ratio, in the presence of $NaBPh_4$, affords deep brown crystals of formula $[(triphos)Co(N_3)]_2(BPh_4)_2 \cdot 2(CH_3)_2CO$. When the reaction is performed with a metal/azido 1:2 molar ratio, deep brown crystals of formula $(triphos)Co(N_3)_2$ are obtained.

Both the complexes slowly decompose in the air. $[(triphos)Co(N_3)]_2(BPh_4)_2 \cdot 2(CH_3)_2CO$ behaves as a 1:2 electrolyte in nitroethane solution, whereas $(triphos)Co(N_3)_2$ is not an electrolyte. The IR spectra of both complexes, in Nujol mulls, show one band at 2060 (s) cm^{-1} and two bands (s, m) at 2060 and 2030 cm^{-1}, respectively, attributed to N_3 stretching vibrations. The electronic spectra show a broad band at 11 100 cm^{-1} with a shoulder at 8700 cm^{-1}.

The molecular structure of $[(triphos)Co(N_3)]_2(BPh_4)_2 \cdot 2(CH_3)_2CO$ consists of dinuclear $[(triphos)_2Co_2(N_3)_2]^{2+}$ cations, BPh_4^- anions, and acetone solvating molecules. A perspective view of the complex cation is shown in Figure 1, and selected bond

(18) Corfield, P. W. R.; Doedens, R. J.; Ibers, J. A. *Inorg. Chem.* **1967**, *6*, 197.
(19) (a) Stewart, J. M.; Kundall, F. A.; Baldwin, J. C. "X-Ray System of Programs"; Technical Report TR 192; University of Maryland: College Park, MD, 1972. (b) Sheldrik, G. "SHELX-76 System of Computing Programs"; University of Cambridge: Cambridge, England, 1976. (c) Johnson, C. K. "ORTEP"; Report ORNL-3794; Oak Ridge National Laboratory: Oak Ridge, TN, 1965.
(20) *International Tables for X-Ray Crystallography*; Kynoch: Birmingham, England, 1974; Vol. 4, p 71.
(21) Reference 20, p 148.
(22) Hoffmann, R.; Fujimoto, J. R.; Swenson, C.; Wan, C. C. *J. Am. Chem. Soc.* **1973**, *95*, 7644.
(23) O'Connor, C. J.; Cucauskas, E. J.; Deaver, B. S., Jr.; Sinn, E. *Inorg. Chim. Acta* **1979**, *32*, 29.

distances and angles are reported in Table IV.

In the complex cation two symmetrically related (triphos)Co^{2+} moieties are bridged by two end-to-end azide groups. The eight-membered $Co_2(\mu\text{-}N_3)_2$ cycle is planar within 0.16 Å, the Co–Co distance being 5.06 Å. Each metal atom is five-coordinate by the three phosphorous atoms of the tripod ligand and by two nitrogen atoms from two N_3^- groups. The overall geometry around each cobalt atom can be described as distorted square pyramidal with basal angles of 156.3 (3) and 158.5 (3)°.

The Co–P bond distances, ranging from 2.207 (3) to 2.261 (3) Å, are fully comparable with those reported for square-pyramidal Co(II) complexes. The Co–P bonds trans to the azido groups are shorter (average 2.215 Å) than the other one (2.261 (3) Å). The azide bridges are slightly asymmetric, with the two Co–N–N angles of 124.5 (8) and 139.4 (9)° and with bond distances of 1.917 (9) and 1.945 (9) Å, respectively.

Magnetic Behavior. The magnetic behavior of [(triphos)Co(N_3)]$_2$(BPh_4)$_2$·2(CH_3)$_2$CO has been investigated both with variable-temperature magnetic susceptibility measurements and EPR spectroscopy. Magnetic susceptibility measurements showed a low value of the magnetic moment, $\mu_{eff} \approx 1.4\ \mu_B$, constant in the temperature range 300–4.3 K. This is indicative of a Curie behavior, which can be ascribed to a monomeric species. The exact value of the magnetic moment was found to depend on actual sample, ranging from 0.8 to 1.6 μ_B in all the samples we have examined. The EPR spectra showed only a very weak feature at $g \approx 2.15$ or no signal at all depending on the sample we used.

From the above data we concluded that the compound is diamagnetic with a variable amount of paramagnetic impurities probably due to formation of monomeric species of the type [(triphos)Co(N_3)$_2$].

Orbital Nature of the Exchange Interaction. When no direct metal–metal bond occurs, the exchange interaction between paramagnetic centers in complexes is due to the delocalization of the magnetic electrons onto orbitals of the ligands that connect the centers themselves.[24] This exchange mechanism, which is also called superexchange, has been thoroughly studied in the last few years mainly by using orbital models based on extended Hückel[25-27] or ligand field formalisms.[28] From the interaction between two paramagnetic centers with one unpaired electron on each center, two spin states occur: a singlet ($S = 0$) diamagnetic and a triplet ($S = 1$) paramagnetic state. In the orbital model the singlet–triplet separation, J is written as

$$J = J_F + J_{AF} \tag{1}$$

where J_F is a ferromagnetic contribution that stabilizes the $S = 1$ state, and J_{AF}, the antiferromagnetic contribution, stabilizes the diamagnetic ground state. J_F and J_{AF} are related to the nature of the magnetic oribtals ϕ_a and ϕ_b and to the molecular orbitals that originate from them, ϕ_1 and ϕ_2, by

$$J_F = -K_{ab} \tag{2}$$

$$J_{AF} = (\epsilon_1 - \epsilon_2)^2/(J_{aa} - J_{ab}) \tag{3}$$

where ϵ_i is the Hartree–Fock energy of the ith orbital obtained from a SCF calculation on the triplet state and K_{ab}, J_{aa}, and J_{ab} are exchange and Coulomb integrals. The energy difference ($\epsilon_1 - \epsilon_2$) can be evaluated within the extended Hückel or the ligand field formalism for any set of geometrical and bonding parameters. It has been generally observed that large $|\epsilon_1 - \epsilon_2|$ values stabilize the diamagnetic singlet states.[9,29] Small $|\epsilon_1 - \epsilon_2|$ values, however, do not necessarily mean that the triplet state is the ground state. In order to have J_F contributions to J, in fact, K_{ab} must be different from zero.[9] The K_{ab} value is certainly the most difficult quantity to evaluate, and more complex mechanisms, such as double-spin polarization, metal–ligand and ligand–metal charge transfer, etc., have been included in the theoretical treatment.[9,10,30]

In copper type I complexes the J_{AF} term was found to be dominant, thus determining the singlet ground state,[9] while in type II complexes double-spin polarization effects were found to determine a large negative J_F value.[9,10]

The energy level diagram we obtain from the extended Hückel calculations is shown in Figure 2. On the left the orbitals for a $(N_3)_2^{2-}$ fragment are shown; on the right the ten metal d orbitals of the $(Co_2)^{4+}$ fragment are plotted. In the center we show the computed highest occupied and lowest unoccupied molecular orbitals, a_u, a_g, b_u, and b_g, of the whole molecule. The linear combinations of the fragment molecular orbitals are schematically represented on the extreme sides of the figure. In our model complex of C_{2h} symmetry the HOMO's are the a_g and b_u molecular orbitals, which originate from the d_{z^2} metal orbitals. They are separated by 0.14 eV by interaction with the out-of-plane a_g and b_u orbitals of the $(N_3)_2^{2-}$ fragment. A much larger interaction is experienced by the b_g and a_u LUMO's, which are split by 0.64 eV. These orbitals are mainly $d_{x^2-y^2}$ in nature, and they can strongly interact with the in-plane a_u and b_g orbitals of the $(N_3)_2^{2-}$ fragment. Extended Hückel calculations on copper(II) type I complexes, in which the a_u and b_g orbitals are the HOMO's, gave a splitting of 1.1 eV, which was claimed to explain the observed diamagnetism of the complexes.[7]

It is apparent that the above results are not fully consistent with the observed diamagnetism of [(triphos)Co(N_3)]$_2$(BPh_4)$_2$·2(CH_3)$_2$CO. It must be remembered, however, that in the above calculations we used an idealized symmetry. The actual symmetry of the complex is in fact only C_i. In this symmetry the d_{z^2} and $d_{x^2-y^2}$ orbitals can admix and the resulting magnetic orbitals are a mixture of the two. This low symmetry effect is responsible for an increase in the $|\epsilon_1 - \epsilon_2|$ energy difference and can thus explain the observed diamagnetism of the present complex.

A schematic view of the [LNi(μ-N_3)$_3$NiL]$^+$ cation is shown in Figure 3. It is apparent that one of the main deviation from the normal bonding geometry of the azido groups is the noncopolanarity of the two in-plane N_3^- groups and the equatorial planes of the nickel(II) ions. Since this geometrical deformation is expected to influence the overlap between the $d_{x^2-y^2}$ and the p in-plane orbitals, we performed an extended Hückel calculation on our model complex allowing for the noncoplanarity of the $(N_3)_2$ and the CoP_2N_2 planes. For a dihedral angle of 20° a splitting of 0.39 eV is computed between the b_g and a_u orbitals, which is 0.6 times the splitting computed in the coplanar situation. From these calculations it follows that deviations from the coplanarity can strongly influence the exchange pathway in μ-azido-bridged complexes. It should be noted at this point that a quantitative explanation of the actual values of the coupling constants observed in the present complex and the nickel ones is not possible on these grounds. A quantitative estimate of the J values has been successfully done in a number of cases, and it would require more sophisticated calculations at the SCF level.[29-32] The present results can however be used to rationalize the overall trend in J values. On passing from copper(II) to nickel(II) complexes, one should in principle expect not a large variation in the strength of the exchange interaction since the largest contribution to the exchange pathway comes from the $d_{x^2-y^2}$ or d_{xy} orbitals unless some distortion from the coplanarity of the M(μ-N_3)$_2$M moiety occurs. As a matter of fact, following these lines, a decrease in the J value can be anticipated for [LNi(μ-N_3)$_3$NiL]ClO_4 as compared to [L'Ni(N_3)(μ-N_3)$_2$Ni(N_3)L'] since in the latter structure the deviation of M(μ-N_3)$_2$M from coplanarity is less pronounced.[16]

Conclusions

The exchange interactions between paramagnetic transition-

(24) Anderson, P. W. *Magnetism*; Rado, G. T., Suhl, H., Eds.; Academic Press: New York, 1963; Vol. 1, p 99.
(25) Hay, P. J.; Thibeault, J. C.; Hoffmann, R. *J. Am. Chem. Soc.* **1975**, *97*, 4884.
(26) Kahn, O.; Briat, B. *J. Chem. Soc., Faraday Trans. 2* **1976**, *72*, 268.
(27) Kahn, O.; Briat, B. *J. Chem. Soc., Faraday Trans. 2* **1976**, *72*, 1441.
(28) Bencini, A.; Gatteschi, D. *Inorg. Chim. Acta* **1978**, *31*, 11.
(29) Albonico, C.; Bencini, A. *Inorg. Chem.* **1978**, *27*, 1934.
(30) De Loth, P.; Cassoux, P.; Daudey, J. P.; Malrieu, J. P. *J. Am. Chem. Soc.* **1981**, *103*, 4007.
(31) Bencini, A.; Gatteschi, D. *J. Am. Chem. Soc.* **1986**, *108*, 5763.
(32) Noodleman, L.; Baerends, E. J. *J. Am. Chem. Soc.* **1984**, *106*, 2316.

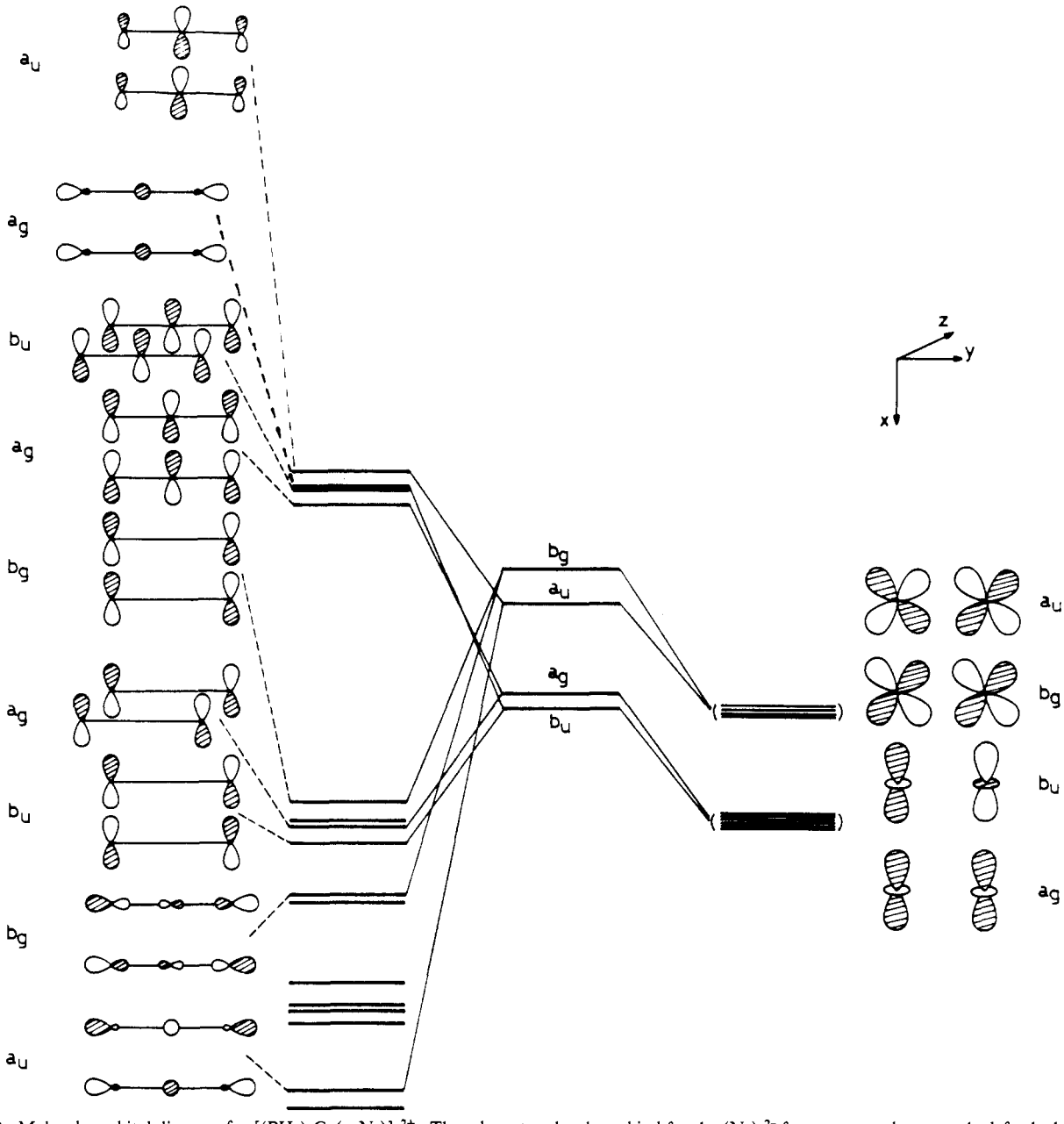

Figure 2. Molecular orbital diagram for $[(PH_3)_3Co(\mu\text{-}N_3)]_2^{2+}$. The relevant molecular orbital for the $(N_3)_2^{2-}$ fragment are shown on the left; the highest occupied and the lowest unoccupied 3d metal orbital of the $(Co_2)^{4+}$ are shown on the right; the highest occupied (a_g, b_u) and lowest unoccupied (a_u, b_g) molecular orbitals of the dimer are shown in the center.

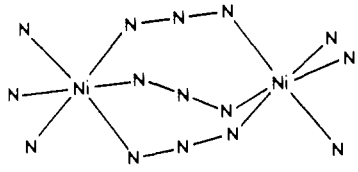

Figure 3. Schematic representation of the structure of the $[LNi(\mu\text{-}N_3)_3NiL]^+$ cation (L = *N,N',N''*-trimethyl-1,4,7-triazacyclononane).

metal ions propagated through azido bridges are strongly dependent on the bridging mode of the N_3^- ions. When the azido groups are bridging in the end-to-end mode, the exchange interaction is always ferromagnetic when the magnetic electrons are in an in-plane $d_{x^2-y^2}$ or d_{xy} orbital. In the present complex $[(triphos)Co(\mu\text{-}N_3)]_2(BPh_4)_2$ the observed diamagnetism has been rationalized through a low-symmetry mixing of d_{xy} and d_{z^2} metal orbitals by using extended Hückel calculations. With these calculations it has been also found that deviations of the $M(\mu\text{-}N_3)_2M$ moiety from coplanarity can influence the strength of the magnetic interactions, and the trend in the *J* values observed in two azido-bridged nickel(II) complexes has been rationalized.

Acknowledgment. Thanks are expressed to Franco Cecconi and Aldo Traversi, ISSECC-CNR, for technical assistance.

Registry No. $[(triphos)Co(N_3)]_2(BPh_4)_2\cdot 2(CH_3)_2CO$, 119638-36-7; $[(triphos)Co(N_3)_2]$, 119638-37-8; $\{[(PH_3)_3Co]_2(N_3)_2\}^{2+}$, 119638-39-0; $[LNi(\mu\text{-}N_3)_3NiL]^+$, 119638-38-9.

Supplementary Material Available: Tables SI–SIV, listing crystal data and data collection details, derived positional parameters of group atoms, derived hydrogen positional parameters, and thermal parameters (7 pages); a table of calculated and observed structure factors (22 pages). Ordering information is given on any current masthead page.